



HAL
open science

Eddy Viscosity in Dense Granular Flows

Thomas G Miller, P Rognon, B Metzger, I Einav

► **To cite this version:**

Thomas G Miller, P Rognon, B Metzger, I Einav. Eddy Viscosity in Dense Granular Flows. Physical Review Letters, 2013, 111, pp.058002. 10.1103/PhysRevLett.111.058002 . hal-01442075

HAL Id: hal-01442075

<https://hal.science/hal-01442075>

Submitted on 20 Jan 2017

HAL is a multi-disciplinary open access archive for the deposit and dissemination of scientific research documents, whether they are published or not. The documents may come from teaching and research institutions in France or abroad, or from public or private research centers.

L'archive ouverte pluridisciplinaire **HAL**, est destinée au dépôt et à la diffusion de documents scientifiques de niveau recherche, publiés ou non, émanant des établissements d'enseignement et de recherche français ou étrangers, des laboratoires publics ou privés.

Eddy Viscosity in Dense Granular Flows

T. Miller,¹ P. Rognon,^{1,2} B. Metzger,² and I. Einav^{1,3,*}

¹Particles and Grains Laboratory, School of Civil Engineering, The University of Sydney, Sydney, New South Wales 2006, Australia

²IUSTI-CNRS UMR 7343, Aix-Marseille University, 13453 Marseille, France

³Department of Civil, Environmental and Geomatic Engineering, Faculty of Engineering Science, University College London, London WC1E 6BT, United Kingdom

(Received 9 November 2012; published 2 August 2013)

We present a seminal set of experiments on dense granular flows in the stadium shear geometry. The advantage of this geometry is that it produces steady shear flow over large deformations, in which the shear stress is constant. The striking result is that the velocity profiles exhibit an *S* shape, and are not linear as local constitutive laws would predict. We propose a model that suggests this is a result of wall perturbations which span through the system due to the nonlocal behavior of the material. The model is analogous to that of eddy viscosity in turbulent boundary layers, in which the distance to the wall is introduced to predict velocity profiles. Our findings appear pivotal in a number of experimental and practical situations involving dense granular flows next to a boundary. They could further be adapted to other similar materials such as dense suspensions, foams, or emulsions.

DOI: [10.1103/PhysRevLett.111.058002](https://doi.org/10.1103/PhysRevLett.111.058002)

PACS numbers: 45.70.Mg, 81.05.Rm, 83.10.Bb, 83.50.Ax

Dense granular flows exhibit complex properties that challenge unified description. For the last decade, major advances have been made towards the expression of a local constitutive law. Within flows in various geometries the local shear strain rate $\dot{\gamma}$ and the local shear stress τ were found to satisfy the Bagnold scaling $\tau = \rho d^2 f_1(\phi) \dot{\gamma}^2$ [1], involving the grain size d , density ρ , and a function f_1 that diverges as the solid fraction ϕ approaches a maximum value. However, the constitutive law that describes the bulk flow does not usually apply close to walls. In fact, there can be significant deviation from the Bagnold scaling over large distances—possibly spanning through the entire flow. Therefore, predicting flows not only requires the knowledge of the constitutive law but also that of a law describing the wall perturbation. No consensus has yet emerged on the general form of such a law of the wall for dense granular flows.

A fascinating property of dense granular flows is the spontaneous development of transient collective grain motions [2–10]. By making analogies with turbulent eddies these phenomena were termed granulence [3]. As opposed to turbulent eddies, the typical size ℓ of these structures tends to increase and diverge as the flow slows down and jams. Local constitutive laws were reformulated introducing this mesoscopic length scale ℓ in place of the grain size d . This gave a consistent prediction for the viscosity divergence when approaching the jamming [2,5,7,11].

These correlated structures lead to an even deeper reformulation of the flow description, using nonlocal models. The underlying idea is that the behavior at a given point in the flow depends on the nature of the flow in the surrounding region, which is given by some typical cooperativity length. Two main models were introduced, considering either nonlocal self-activated processes [12], or nonlocal

fluidity [13]. These models significantly improved the prediction of local rheology in flows involving stress gradients such as cylindrical Couette flows and flows down a slope. Despite these advances, these models are not conclusive on the role of walls and the flow perturbations they may induce.

In this Letter, we present a seminal set of experiments revealing long-range wall perturbation in dense granular flows. Results suggest a simple model that consists of introducing the distance to the wall as a typical length scale for the diffusion of momentum. This model is similar to the eddy viscosity model and its application to derive the law of the wall in turbulent boundary layers.

S-shaped velocity profile in plane shear flows.—For this study we designed an original experimental device named stadium shear that can produce plane shear of a 2D granular material (see Fig. 1). The grains are 10 mm high nylon cylinders of three different diameters (12, 15, and 20 mm) to prevent crystallization. They stand on a glass plate, and the flow is driven by a belt system. The nylon-faced rubber belt has asperities that are semicircular in cross section with a 6 mm radius and a center-to-center spacing of 14 mm. Grains are sheared between two parallel sections of the belt in the central region and recirculate underneath the sprockets at both ends. The advantage of this setup is the ability to have plane shear in the central region while the recirculation of the particles allows continuous shear for deformations as large as desired. The 2D nature of the granular system allows individual particles in the plane shear region (see Fig. 1) to be tracked by a high-speed camera which sits above the apparatus. From consecutive images—and using a circular Hough transformation algorithm—the displacement of the grains over time can be obtained. The normal stress acting on the central region of the belt is measured

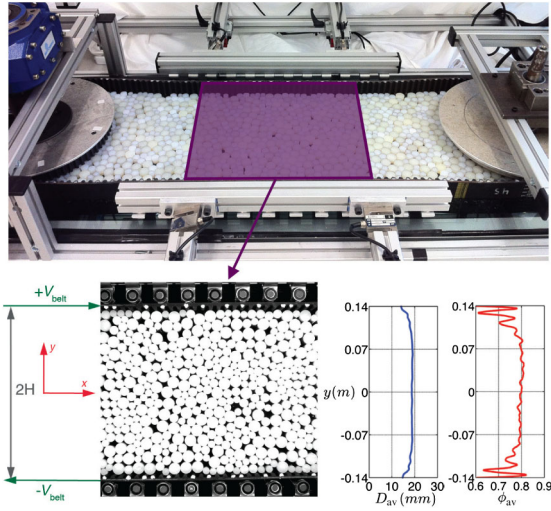


FIG. 1 (color online). Stadium shear device: 2000 plastic cylinders set on a glass plate are sheared by a belt system. Time averaged profiles ($V^{\text{belt}} = 0.1 \text{ m/s}$) of average particle diameter (blue or dark gray) and solid fraction (red or light gray). In the center of the flow, $D_{\text{av}} \approx 18 \text{ mm}$ and $\phi_{\text{av}} \approx 0.80$.

through a series of four load cells, one on each arm of the roller assembly (see Fig. 1).

We performed a set of experiments by varying the belt velocity V^{belt} from 1.18 to 11.8 cm s^{-1} , which correspond to a nominal shear rate $\dot{\Gamma} = (V^{\text{belt}}/H)$ between 0.08 and 0.8 s^{-1} . The material was presheared over a deformation of 100 , which was large enough to ensure the system reached a steady state independent of the initial configuration at rest. Images were then recorded over a period of time $100/\dot{\Gamma}$ corresponding to a total shear deformation of 100 . To ensure that particles could be tracked in an effective and efficient manner, the frame rate f of the camera was set so that the maximum displacement between images was less than $0.17d_{\text{min}}$, which corresponds to a shear deformation of 0.012 , and to $f = 0.17V^{\text{belt}}/d_{\text{min}}$. Grain velocities are computed by tracking the individual grain position over subsequent frames. The resolution of the images is $r = 2.7$ pixels/mm and the particle tracking algorithm gives subpixel resolution for the grain centers. Considering a typical error of 1 pixel on grain displacement, the typical error on the grain velocity is then $\Delta v = (f/2.7) = (0.17V^{\text{belt}}/2.7d_{\text{min}})$, and the typical error on v_x/V^{belt} is $(0.17/(2.7 \times 12)) \approx 0.5\%$.

For all the runs, we observed that the solid fraction and the average grain size are constant along the flow direction x . They are mostly constant along the shear direction y (see Fig. 1). However smaller grains are slightly segregated toward the layer close to the belt as their size is equal to the size of the belt asperities; they are thus more likely to be trapped by the belt. The average normal stress acting on the central region of the belt increased from 8.81 kPa for $\dot{\Gamma} = 0.08 \text{ s}^{-1}$ to 12.47 kPa for $\dot{\Gamma} = 0.8 \text{ s}^{-1}$. Thus the inertial number [1] $I = (\dot{\gamma}D_{\text{av}}/\sqrt{P/\rho})$ is in the range 5.2×10^{-4} – 4.4×10^{-3} .

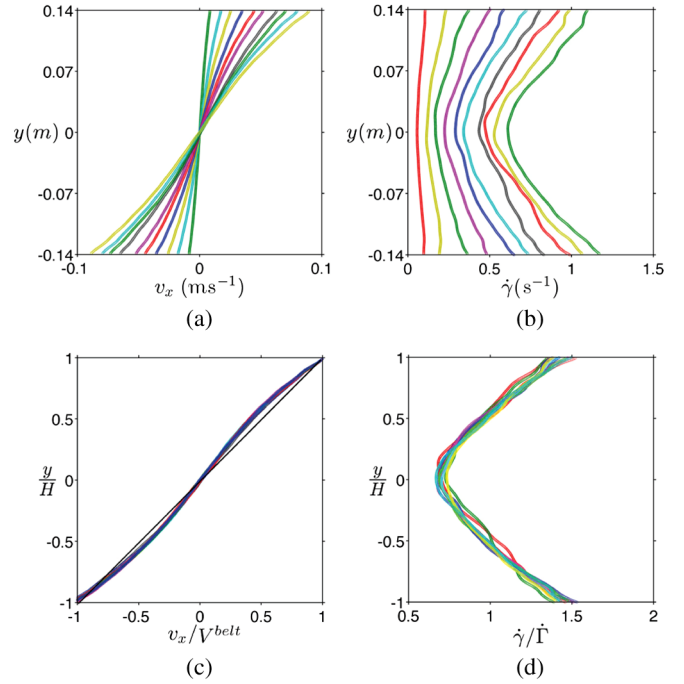


FIG. 2 (color online). (a) Velocity profiles and (b) shear rate profiles for all the runs. The profiles are temporospatial averages of data from the captured central region, which is approximately 368 mm wide, over the entire duration of the test. (c) The normalized velocity profiles and (d) the normalized shear rate profiles (where $\dot{\Gamma} = V^{\text{belt}}/H$). In (c) the linear profile (solid black line) has been included for comparison.

The striking result is the shape of the velocity profile $v_x(y)$, shown in Fig. 2(a). The velocity profiles are not linear; instead they exhibit some curvature. Profiles from all the experiments collapse on to a single S-shaped curve when the velocity $v_x(y)$ is normalized by the belt velocity V^{belt} [see Fig. 2(c)]. The shear rate $\dot{\gamma}(y) = (\partial v_x(y)/\partial y)$ is thus not constant through the flow [see Fig. 2(b)]. It happens to be a minimum at the center of the flow, increasing with proximity to the belt. The magnitude of the variation between the shear rate at the center and at the belt is significant, with a factor of approximately 2 between these values. Like the velocity profiles, the shear rate profiles when rescaled by the nominal shear rate $\dot{\Gamma}$ collapse on to a single curve for all the experiments [see Fig. 2(d)]. As we shall discuss further on, these results appear to be a consequence of the nonlocal behavior of the dense granular flow combined with the presence of walls.

Observation of correlated motions.—The velocity fields for the flows reveal the existence of correlated motions for all shear rates (see Fig. 3), providing further evidence of nonlocal behavior within our system. Individual correlated motions were transient in nature and we observed the ongoing formation and dissipation of such structures throughout each test.

Eddy viscosity and law of the wall.—The stadium shear geometry produces plane shear flows in the central region, which has the advantage of avoiding a stress gradient due

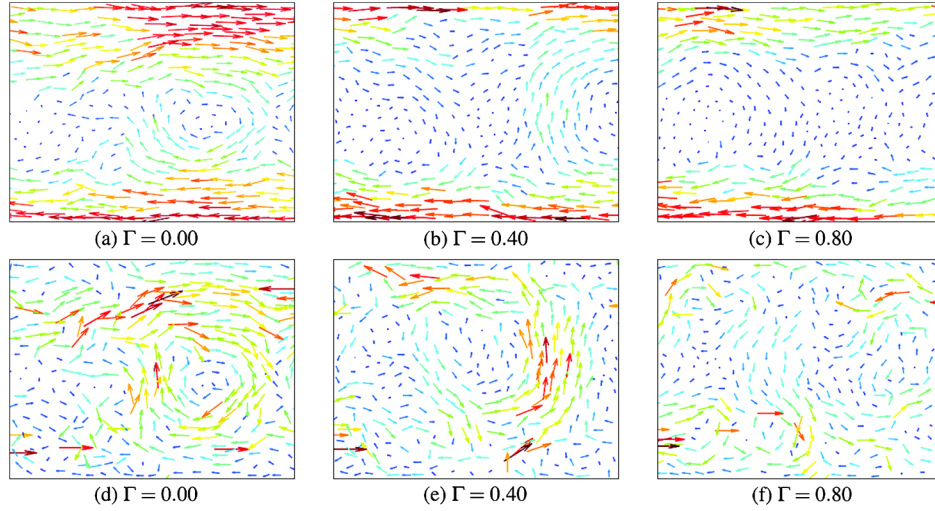


FIG. 3 (color online). (a)–(c) Velocity fields in the steady flow regime during one run ($\dot{\Gamma} = V^{\text{belt}}/H = 0.4 \text{ s}^{-1}$). (d)–(f) Fluctuation velocity fields, where the corresponding shear velocity from the profile in Fig. 2(a) has been subtracted from each vector in (a)–(c). Snapshots are at equal intervals of shear deformation. The arrow color is graded by magnitudes of velocity (with a maximum of $1.03 \cdot V^{\text{belt}}$) and fluctuation velocity (with a maximum of $0.57 \cdot V^{\text{belt}}$), respectively.

to gravity or to a curved geometry. Therefore, unlike flows down a slope or flows in a cylindrical Couette cell, one would expect homogeneity of both the shear stress τ and the normal stress σ . That is, they should not vary along the y direction.

Given that the solid fraction and the grain size are almost constant in the flow (see Fig. 1), any local constitutive law would then predict a constant shear rate $\dot{\gamma}(y)$ along the y direction. For example, the Bagnold scaling [1] $\tau(y) = \rho d^2 f_1(\phi) \dot{\gamma}^2(y)$ predicts $\dot{\gamma}(y) = \sqrt{\tau/\rho d^2 f_1(\phi)}$, which requires a nonconstant stress $\tau(y)$ to obtain a nonconstant shear rate $\dot{\gamma}^2(y)$. Friction between the cylinders and the glass plate could be responsible for such a shear stress gradient. The momentum balance would then read $(\partial\tau/\partial y) = \mu\rho g$, where ρg is the weight per unit volume of the grains, and μ is the coefficient of friction between the grains and the glass. This leads to the prediction that the shear stress linearly increases when moving from the center toward the belt: $\tau(y) = \tau(0) + \mu\rho g|y|$ (the absolute value accounts for the fact that friction forces act against the motion). Using the Bagnold local constitutive law leads to the shear rate profile $\dot{\gamma}^2(y) = \dot{\gamma}^2(0) + (\mu g/d^2 f_1(\phi))|y|$. In this, the predicted increase of shear rate with $|y|$ is qualitatively consistent with the experimental data. However, this expression does not account for the reported scaling of $\dot{\gamma}(y)$ with the belt velocity. This suggests that friction is not responsible for the shape of the shear rate in these experiments. This conclusion finds strong support in Refs. [1,14], which show numerical results from two-dimensional shear flows of grains between two parallel walls. S-shaped velocity profiles were obtained, even in the absence of base friction.

Let us now introduce a model that can explain the curved shape of the shear rate profiles, considering that the shear

stress is constant through the flow. The Bagnold scaling, while being unable to predict such results, relies on an essential idea: the kinematic viscosity scales with $d^2|\dot{\gamma}|$. It suggests that the momentum diffuses at a rate $|\dot{\gamma}|$ over a typical length of one grain size. Given that dense granular flows develop large structures of typical size $\ell \gg d$, one can expect the momentum to transfer over such a distance. This is the core of several models in which the kinematic viscosity scales with $\ell^2|\dot{\gamma}|$ [1,14]. The question is then to establish how this length scale ℓ depends on the flow condition. It happens that ℓ tends to increase as the flow slows down, and can reach very large values. Let us assume that, with our flow conditions, ℓ would tend to be much larger than the flow width H if there were no walls. The presence of the belt thus truncates the maximum distance of momentum diffusion, limiting it to the distance to the wall $H - |y|$. Using this framework, the relationship between shear rate and shear stress at a given location y can be given by

$$\tau = \rho f_1(\phi)(d^2 + a^2(H - |y|)^2)\dot{\gamma}^2(y) \quad (1)$$

with a being a numerical constant. This model then predicts the following shear rate profile:

$$\dot{\gamma}(y) = \dot{\gamma}_H \left(1 + a^2 \left(\frac{H - |y|}{d}\right)^2\right)^{-1/2} \quad (2)$$

with $\dot{\gamma}_H = \dot{\gamma}(H)$ denoting the shear rate at the belt, which according to Eq. (1) is

$$\dot{\gamma}_H = \sqrt{\frac{\tau}{\rho f_1(\phi) d^2}} \quad (3)$$

By definition, the belt velocity is given by $V^{\text{belt}} = \int_0^H \dot{\gamma}(y) dy$. Using Eq. (2) leads to $\dot{\gamma}_H = V^{\text{belt}}/C$, with C a constant that is explicitly defined by the integral

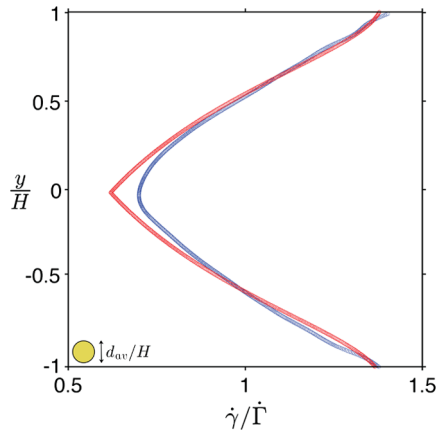


FIG. 4 (color online). The prediction of the model of Eq. (5) with $a = 0.21$ (red or light gray). The normalized average shear rate profile, i.e., the average of the profiles shown in Fig. 2(d) (blue or dark gray).

$$C = \int_0^H \frac{1}{\sqrt{1 + a^2 \left(\frac{H-|y|}{d}\right)^2}} dy = \frac{d}{a} \sinh^{-1} \left(\frac{aH}{d} \right). \quad (4)$$

We can thus write the shear rate profile as

$$\dot{\gamma}(y) = \frac{aV^{\text{belt}}}{d \sinh^{-1}(aH/d)} \left(1 + a^2 \left(\frac{H-|y|}{d} \right)^2 \right)^{-1/2}. \quad (5)$$

At this point, the only unknown parameter is a . It can be determined from experimental values of the shear rate at the belt $\dot{\gamma}_H$ and in the center of the flow $\dot{\gamma}_0 = \dot{\gamma}(0)$, as from Eq. (5) $a = \frac{d}{H} \sqrt{(\dot{\gamma}_H^2 / \dot{\gamma}_0^2) - 1}$. We know that $d/H \approx 0.12$, and Fig. 2(b) indicates that $(\dot{\gamma}_H / \dot{\gamma}_0) \approx 2$, leading to a value for a : $a \approx 0.21$. Figure 4 shows the model prediction against the normalized average shear rate from the experiments. The model captures the scaling of $\dot{\gamma}(y)$ with the belt velocity V^{belt} (i.e., $\dot{\gamma}(y) \propto V^{\text{belt}}$).

Conclusions.—The stadium shear experiments we presented in this Letter revealed an important feature of dense granular flows: even in the absence of a stress gradient, the shear rate significantly increases when approaching the walls. This property is central to many applications involving granular flows near a solid boundary. This includes tribology and the prediction of basal sheared layers of landslides or snow avalanches. It also seems that such long-range wall effects should be considered to refine the interpretation of experimental granular flows in Couette cells, and thin granular layers flowing down a slope.

The model we suggested to describe the long-range wall effect of the shear rate is analogous to the eddy viscosity model used to predict the velocity profiles in boundary layers of turbulent flows. Our model is also based on the idea that the transfer of momentum could occur over large length scales if it was not truncated by the presence of a wall. This is therefore a nonlocal model. It could

complement existing nonlocal models which have mainly focused on the effect of a stress gradient in the bulk flow.

Our experimental study covered a range of shear rates in a fixed geometry condition for a particular system width H , and a particular solid fraction. Velocity profiles always exhibited S shapes. It may be expected that different flow conditions could lead to more or less linear profiles. They could for instance lead to different values of the parameter a , thereby tuning the relative effect of the eddy viscosity to the local viscosity.

This work may be useful in understanding the existence of vortices within shear bands, such as those observed recently in sands [15]. Also, long-range wall effects are thought to exist in other particulate systems, such as dense suspensions, foams, and emulsions. Given that the proposed model only involves the system size, it is hoped that it could be adapted to them by considering their specific local constitutive law.

*Corresponding author.

itai.einav@sydney.edu.au

- [1] GDR MiDi, *Eur. Phys. J. E* **14**, 341 (2004); Y. Forterre and O. Pouliquen, *Annu. Rev. Fluid Mech.* **40**, 1 (2008).
- [2] D. Ertas and T.C. Halsey, *Europhys. Lett.* **60**, 931 (2002).
- [3] F. Radjaï and S. Roux, *Phys. Rev. Lett.* **89**, 064302 (2002).
- [4] F. Radjaï and S. Roux, in *Nonsmooth Mechanics and Analysis*, edited by P. Alart, O. Maisonneuve, and R.T. Rockafellar, Advances in Mechanics and Mathematics Vol. 12 (Springer, New York, 2006), pp. 233–245.
- [5] O. Pouliquen, *Phys. Rev. Lett.* **93**, 248001 (2004).
- [6] A.V. Orpe and A. Kudrolli, *Phys. Rev. Lett.* **98**, 238001 (2007).
- [7] P. Mills, P. Rognon, and F. Chevoir, *Europhys. Lett.* **81**, 64005 (2008).
- [8] P. Rognon and I. Einav, *Phys. Rev. Lett.* **105**, 218301 (2010).
- [9] P. Chaudhuri, V. Mansard, A. Colin, and L. Bocquet, *Phys. Rev. Lett.* **109**, 036001 (2012).
- [10] V. Richefeu, G. Combe, and G. Viggiani, [arXiv:1208.0485](https://arxiv.org/abs/1208.0485).
- [11] C. Bonnoit, T. Darnige, E. Clement, and A. Lindner, *J. Rheol.* **54**, 65 (2010); C. Bonnoit, J. Lanuza, A. Lindner, and E. Clement, *Phys. Rev. Lett.* **105**, 108302 (2010).
- [12] O. Pouliquen and Y. Forterre, *Adv. Compl. Syst.* **04**, 441 (2001); *Phil. Trans. R. Soc. A* **367**, 5091 (2009).
- [13] J. Goyon, A. Colin, G. Ovarlez, A. Ajdari, and L. Bocquet, *Nature (London)* **454**, 84 (2008); K. Kamrin and G. Koval, *Phys. Rev. Lett.* **108**, 178301 (2012).
- [14] F. da Cruz, F. Chevoir, J.N. Roux, and I. Iordanoff, in *Transient Processes in Tribology*, edited by G. Dalmaz, A.A. Lubrecht, D. Dowson, and M. Priest (Elsevier, New York, 2004), pp. 53–61.
- [15] S. Abedi, A.L. Rechenmacher, and A.D. Orlando, *Granular Matter* **14**, 695 (2012).